Tidal energy extraction in three-dimensional ocean models

Goward Brown, Alice; Neill, Simon; Lewis, Matthew

Renewable Energy

DOI:
10.1016/j.renene.2017.04.032

Published: 01/12/2017

Peer reviewed version

Tidal energy extraction in three-dimensional ocean models

Alice J. Goward Brown*, Simon P. Neill, Matthew J. Lewis

School of Ocean Sciences, Menai Bridge, Bangor, Gwynedd, LL59 5AB, UK

A B S T R A C T

Access to high performance computing has made 3-D modelling de rigueur for tidal energy resource assessments. Advances in computing resources and numerical model codes have enabled high resolution 3-D ocean models to be applied at basin scales, albeit at a much higher computational cost than the traditional 2-D modelling approach. Here, a comparison between 2-D and 3-D tidal energy extraction modelling techniques is undertaken within a 3-D modelling framework, and differences between the methods are examined from both resource and impact assessment perspectives. Through a series of numerical experiments using the Regional Ocean Modeling System (ROMS), it is shown that 3-D tidal energy extraction can be successfully incorporated in a regional ocean model of the Pentland Firth - one of the top regions in the world for tidal stream energy development. We demonstrate that resolving 3-D flow is important for reducing uncertainty in environmental resource assessments. Further, our results show that 2-D tidal energy extraction methods lead to a misrepresentation of the velocity profile when applied to 3-D models, demonstrating the importance of resolving 3-D flows in the vicinity of tidal arrays.

1. Introduction

When identifying a tidal energy site, the water depth, proximity to a grid connection and an energetic resource (peak spring tidal flows in excess of 2 m/s) are the main characteristics considered [9,11]. Tidal currents are three-dimensional, and contain non-linear features (i.e turbulence, eddy fields and overtides), hence, in order to properly characterise the available resource, hub-height velocities should be used for characterisation of inflow conditions [34]. In tidal stream energy applications, current speed information is required to predict the forces on the turbine and power output. In first generation tidal stream, shallow water (<100 m) environments, the fastest tidal currents are found between the middle and surface of the water column [35], subsequently tidal stream turbines are designed to extract the flow in the upper reaches of the water column [7]. Modelling tidal energy extraction poses a multi-scale challenge to the tidal energy research community [2], turbine scale - the hydrodynamic flow between individual devices and array scale - the interaction of the tidal stream hydrodynamics with the entire array, where the research question posed ultimately dictates the suitability of the methods used. Traditionally, three-dimensional (3-D) Computational Fluid Dynamics (CFD) models have been employed to study individual turbines, whereas two-dimensional (2-D) modelling techniques have been used for large array scale modelling, with turbines represented using the actuator disc concept applied as an area of enhanced drag stress within a regional model [36,13,3,32]. More recently, researchers have begun using 3-D models to assess the theoretical resource of regions [24,50] and assess the potential impacts of tidal energy extraction [29]. Computational advancements have made tidal energy extraction feasible within regional 3-D models. For accurate resource assessments, it is necessary to include the interaction of the tidal stream with the tidal array [10], since the extraction of tidal energy will lead to changes within the velocity structure [29,49]. The use of depth-averaged velocities is therefore inaccurate for resource assessments because the velocity profile in a realistic case will be distorted, such that the velocities across the swept area of the rotor will be less than those above and below the device. Accurately defining the flow around the turbine will reduce uncertainty in resource calculations. The increase in turbulence and the velocity deficit caused by upstream turbines will impact the turbine yield downstream. Turbine wake comparisons between flume experiments and CFD actuator disc models show similar characteristics [18]. It is hypothesised that flow bypass around the turbine will change the projected resource from that calculated by a depth-averaged model.

* Corresponding author.
E-mail address: a.j.gowardbrown@bangor.ac.uk (A.J. Goward Brown).

1.1. Impact assessments

Environmental impact assessments have identified a number of key physical and biological parameters which could be affected by feedbacks between in-stream tidal energy extraction and the local hydrodynamics. Namely: flow hydrodynamics, sediment dynamics, artificial reef effects and habitat disruption caused by the installation, operation and maintenance of devices [42,40], the impacts of which have yet to be successfully quantified. In the region of the array, 2-D extraction methods will reduce velocities over the whole water column. In reality the tidal current will increase around the tidal stream device [5,27], which is reproducible using a 3-D method [38]. Research by Vogel et al. [46]; identifies that in order to match the total power removed by a 2-D array to that removed by a 3-D array, the 2-D model requires a lower thrust to be applied to the flow than the 3-D simulation, which would lead to a higher flow speed through the array. Additionally, previous methods where an enhanced bed friction is used to represent tidal stream turbines in a 3-D model will ultimately misrepresent the vertical flow bypass around the device (i.e [29]; Fig. 1). With the 2-D method there will be a higher bottom drag associated with the region of the array, which will have consequences for sediment transport applications.

The aim of this research is to use a three dimensional (3D) hydrodynamic model to quantify the differences between using depth-averaged and 3-D numerical methods for tidal energy extraction, in order to help reduce uncertainty within resource and environmental impact assessments and to highlight when a 3-D resource assessment is required. Tidal stream extraction is included in the numerical model using a methodology based on that developed by Roc et al. [38] which applies the actuator disc concept to the 3D Regional Ocean Modeling System (ROMS). The paper applies both methods to an idealised model of an energetic tidal channel to examine the reliability of depth-averaged tidal extraction methods when water depth is increased between the upper and lower limits of first generation tidal energy sites (Section 3). The methods are then applied to a regional model of the Pentland Firth and the impact of each method on the flow-field is explored from an environmental impact assessment perspective. The Pentland Firth has a world-leading tidal stream resource and hence is of great interest to UK tidal energy development [26]. The environmental impact focus will be on changes to flow behavior with a view to future works on impacts to sediment dynamics. Sandbanks are important coastal features which are valuable to the aggregate and fishing industries and also naturally protect coastlines through the dissipation of wave energy [29].

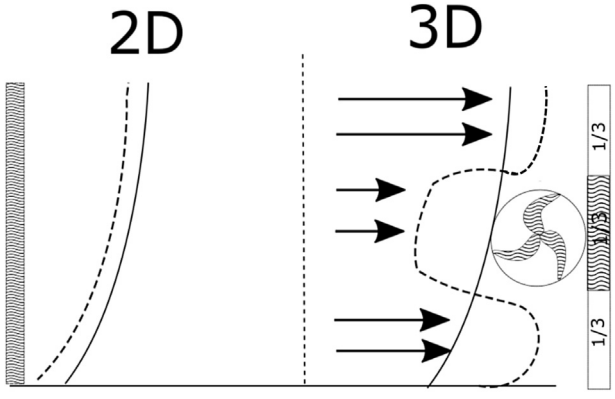

Fig. 1. Illustrated comparison of the consequent vertical tidal current profiles if 2-D (solid line) or 3-D (dashed line) turbine modelling methods are used in 3-D ocean models.

2. Numerical modelling

This study used the Regional Ocean Modeling System (ROMS), to compare tidal energy extraction methodologies. ROMS has been used in recent publications of resource assessments [45,24,37]. However, these works have not considered the variability of the tidal current resource over the water column. Tidal energy extraction is paramaterised within the ROMS source code using a method developed by Roc et al. [38]; described in Section 2.2.

2.1. ROMS

ROMS (Regional Ocean Modeling System) is an open-source 3-D model which solves the hydrostatic Navier-Stokes equations using a Boussinesq approximation on a structured horizontal grid with terrain following sigma layers [41]. ROMS undergoes continuous development by its active user community led by Rutgers University and the University of California, Los Angeles (www.myroms.org). It is suitable for a wide range of applications, over a variety of scales from idealised analytical studies [45] to coastal and regional domains [31], toolboxes have been created to couple ROMS with various models, such as the wave model SWAN and sediment sub-models [47].

2.2. Modelling tidal energy extraction

In this study, an external force (F_t) is applied to the ROMS momentum equations to simulate the impact of tidal energy extraction (Equation (1)) [39]. The force of a turbine acting on the fluid (F_t) is defined by Equation (2), where C_t is the dimensionless thrust coefficient, related to the porosity of the disc by the induction factor a. a, is a dimensionless quantity ranging between 0 and 1 which represents the reduction in flow velocity [19].

In order to account for realistic flow conditions, it is more accurate to define F_t as a function of the flow velocity at the disk location ($\overrightarrow{U_d}$) instead of the unconstrained upstream velocity (U_∞), in order for flow interaction with the turbine structure to be taken into account.

$$\begin{cases} \frac{\delta u}{\delta t}+\vec{v}\cdot\nabla u-fv=-\frac{\delta\phi}{\delta x}-\frac{\delta}{\delta z}\left(-K_M\frac{\delta u}{\delta z}-\nu\frac{\delta u}{\delta z}\right)+A_M\left(\frac{\delta^2\bar{u}}{\delta x^2}+\frac{\delta^2\bar{v}}{\delta y^2}\right)+\frac{1}{2}F_t \\ \frac{\delta v}{\delta t}+\vec{v}\cdot\nabla v+fu=-\frac{\delta\phi}{\delta y}-\frac{\delta}{\delta z}\left(-K_M\frac{\delta v}{\delta z}-\nu\frac{\delta v}{\delta z}\right)+A_M\left(\frac{\delta^2\bar{v}}{\delta x^2}+\frac{\delta^2\bar{u}}{\delta y^2}\right)+\frac{1}{2}F_t \end{cases} \quad (1)$$

A_M represents the horizontal eddy viscosity, K_M the vertical viscosity, u, v are the velocity components in x and y respectively. z is the water depth, $\vec{v}$ is the mean velocity vector and f is the coriolis parameter. ϕ is the dynamic pressure which is equal to the total pressure, P, divided by the background density ρ_0. F_t is the force being applied over the turbine swept area (A_D), characterised by the dimensionless thrust coefficient C_t (Equation (2)).

$$C_t=\frac{F_t}{\frac{1}{2}\rho A_D U_\infty^2}=4a(1-a) \quad (2)$$

Power extraction from the fluid (disregarding any mechanical losses) can be defined as the force multiplied by the rate of work done. According to the definition of the induction factor the extracted power can thus be described as:

$$Power = F_t \times U_d = 2\rho A_d U_\infty^3 a(1-a)^2 \quad (3)$$

For the 3-D extraction method, the force was applied over an area specified in x,y and z directions. A detailed methodology for the implementation of the turbines within the ROMS model can be found in Roc et al. [38]. The 2-D tidal extraction was implemented in the 3-D model by applying the force term over an area in which y was the water column depth and x was the width of the grid cell perpendicular to the dominant flow direction. In this case, the force term was adjusted accordingly to account for the increased area of tidal energy extraction. To ensure the amount of energy extracted by the turbine is equal for both cases the individual input and output velocities were compared (Table 1; Fig. 2). The support structure is neglected in this instance in order to enable the method to be applicable to multiple turbine designs.

The key turbine operating parameters were assumed (Table 1; Myers and Bahaj [27]). This was not an attempt to represent a specific device, however it was intended to represent a typical first-generation tidal stream turbine.

3. Application to an idealised channel

An idealised channel model is created to compare the two methods within an environment which is easily quantifiable. Initially a comparison is made between the two methods to ensure that both methods are reducing the depth-averaged velocities by the same amount, before comparing the velocity profiles and establishing what impacts there might be on resource and environmental impact assessments as a result of these differences (Section 3.2). Finally, both methods are tested in models which become progressively deeper. This final test determines the differing levels of accuracy between the methods in increasingly more complex environments (Section 4).

3.1. Model setup

A channel with dimensions similar to that of the Pentland Firth is simulated (length of 30 km, a width of 20 km). Initially it has a constant depth of 30 m, the lower limit of first generation tidal stream sites. Grid spacing ($\delta x, \delta y$) was equal to 100 m (the diameter of the turbine, plus 5 diameters of spacing either-side) and was 3 m in the vertical to ensure the area of the turbine was resolved by at-least 3 evenly-spaced sigma layers. The lateral boundaries were closed and a free slip condition applied. A constant inflow of 2 m/s was imposed at the upstream channel boundary. The downstream boundary was clamped for depth averaged velocities, and a radiation condition was used for 3-D momentum. The free surface was clamped to enable the comparison of the two methods without the fluctuation of the free-surface. A drag coefficient of 0.0025, similar to other studies of tidal channel [6], was imposed at the bed and the model was run for 48 h, long enough for the model to reach a steady state (where velocities at the turbine location vary less than 1% between each 10 s time-step).

Table 1
Comparison between mid-depth velocity (U) and depth averaged velocity ($\overline{U}$) for both 2-D and 3-D extraction scenarios.

	3-D Method		2-D Method	
	U-velocity	$\overline{U}$ velocity	U-velocity	$\overline{U}$ velocity
T_D (m)	10	10	30	30
U_{IN} (m/s)	2.04	2.00	2.04	2.00
U_{OUT} (m/s)	2.02	1.99	2.03	1.99
U_D (m/s)	1.55	1.81	1.80	1.81

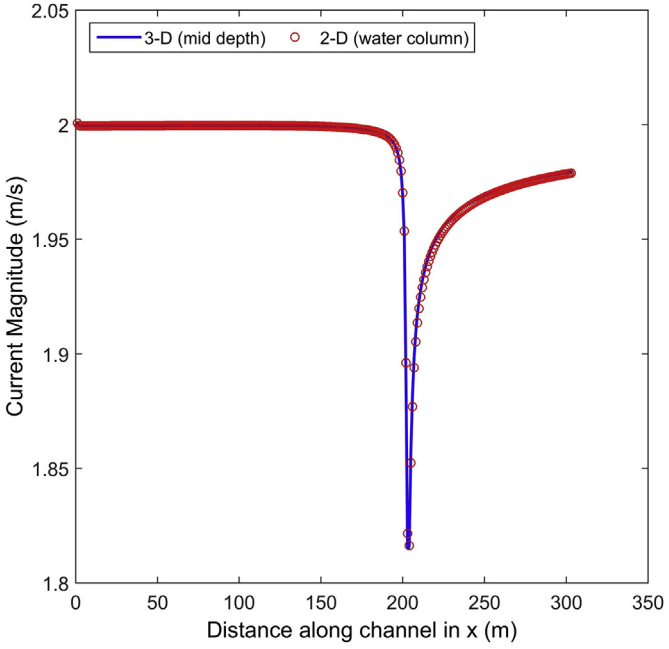

Fig. 2. Comparison of horizontal velocity along the channel domain for both 2-D and 3-D scenarios.

The turbine array is rated at 0.6 MW and has a rated velocity of 2.5 m/s. It is represented by a mid-depth force term (Equation (2)). For 3-D tidal extraction, the height of the turbine (T_D, equivalent to the turbine diameter) is equal to 10 m. For the 2-D extraction case T_D is equal to the water depth (30 m). The array of turbines is located in the middle of the top third of the channel to enable the wake to freely develop; The blockage ratio (B_R), where $B_R = \frac{A_D}{length_{x,y}}$, of the turbine within the channel equates to 5% in x and 3% in y. The area of the turbine, A_D is equal to $\delta x, y \times T_D$.

Adcock et al. [1] recommends boundary lengths of 10 times those of the turbine array. In order to ensure that the model boundaries were sufficiently far from the turbine, multiple model runs were performed with an increasing B_R. The velocities were extracted at the model boundary and compared with a control (no turbine) case to ensure that perturbations resulting from the turbine were not amplified by the boundaries.

3.2. Results: velocity profile

Both the depth-averaged extraction and 3-D extraction reduce the depth-averaged velocity field across the turbine area by 10%, from the input velocity of 2 m/s to 1.8 m/s (Fig. 2). The flow reduction across the 3-D disc is greater (Fig. 3). This discrepancy, which in this case is of the order of 30 cm/s, should be considered when making resource assessments. Wake effects from each method converge approximately 50 turbine diameters downstream of the region of energy extraction however a localised acceleration around the 3-D disc can be observed.

4. Results: idealised tidal energy extraction in deeper water environments

In this scenario, the depth within the idealised channel model is increased from 30 m to 60 m and 90 m (in accordance with typical tidal-stream energy site classifications, Blunden and Bahaj [7]). In each of these three cases, the height (T_D) of the 3-D turbine is increased to maintain a blockage ratio in the vertical of 1/3 [48],

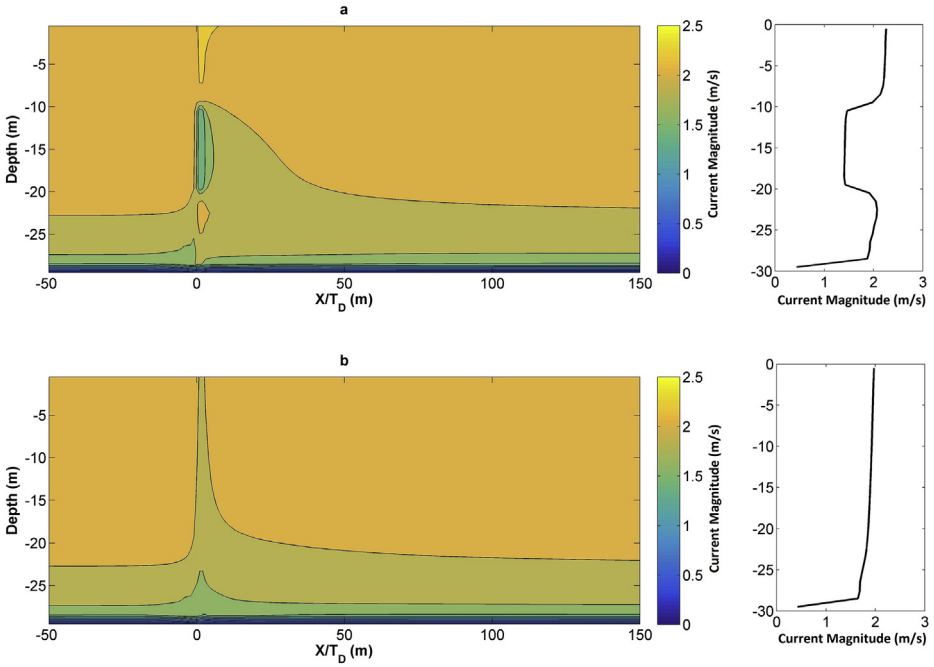

Fig. 3. Vertical flow bypass around the 3-D turbine (a) and through the 2-D turbine (b). X is scaled by the turbine diameter (X/T_D).

and the thrust coefficient altered accordingly. The velocity for all cases remains a constant 2 m/s, forced at the upstream channel boundary. For all cases, both the depth-averaged extraction and 3-D extraction reduce the depth-averaged velocity field from the input velocity of 2 m/s to $\sim$ 1.8 m/s.

4.1. Results: power density

The amount of velocity reduction as a result of tidal energy extraction increases with water depth for the 3-D method, but decreases for the 2-D method (Table 2). The difference in velocity between the scenarios is between 2 and 5 cm/s. The power density (Equation (4)) is calculated for all cases (Figs. 4–6), where Power (P) divided by an area is equal to the kinetic energy (KE) of the flow multiplied by the velocity (u) within the area specified. The results of Figs. 4–6 is summarised in Table 2. It is observed that with the increase in channel depth, the difference between the maximum calculated power density in the channel increases. The difference in calculated power density for the two methods ranges from 1.7 kW/m^2 for the original 30 m channel depth case, to 2 kW/m^2. With the calculated power density for the 2-D case equal to 3298 W/m^2 and 3405 W/m^2 and for the 3-D case the calculated power density across the disc was equal to 1595 W/m^2 and 1406 W/m^2 for the channels with depths of 30 m and 90 m respectively.

$$P/A = KE \cdot u = \frac{1}{2}\rho u^3 \tag{4}$$

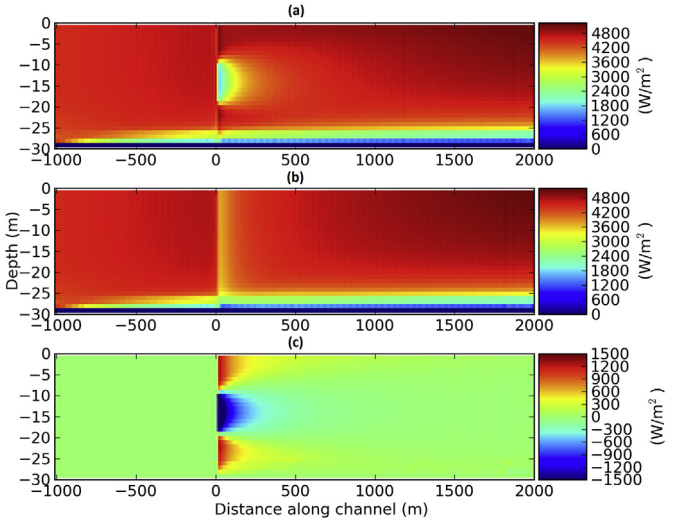

Fig. 4. Power density for (a) the 3-D method, (b) the 2-D method and (c) the power difference between the two methods in a channel of 30 m.

5. Case study – Pentland Firth

The Pentland Firth, an approximately 20 km long channel which separates the Isles of Orkney from the Scottish mainland, connects the North Atlantic Ocean with the North Sea. The tidal dynamics

Table 2
Velocity and power difference between the two methods with increasing channel depth.

Channel depth (m)	Free stream velocity (m/s)	Velocity at turbine (m/s)		Velocity difference (m/s)	Maximum power density difference (kW/m^2)
		2D	3D		
30	2	1.86	1.46	0.4	1.7
60	2	1.87	1.44	0.43	2.2
90	2	1.88	1.4	0.48	2.6

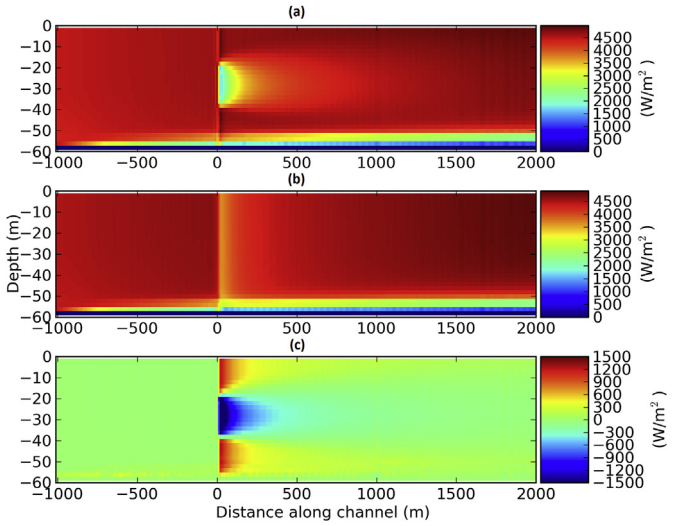

Fig. 5. Power density for (a) the 3-D method, (b) the 2-D method and (c) the power difference between the two methods in a channel of 60 m.

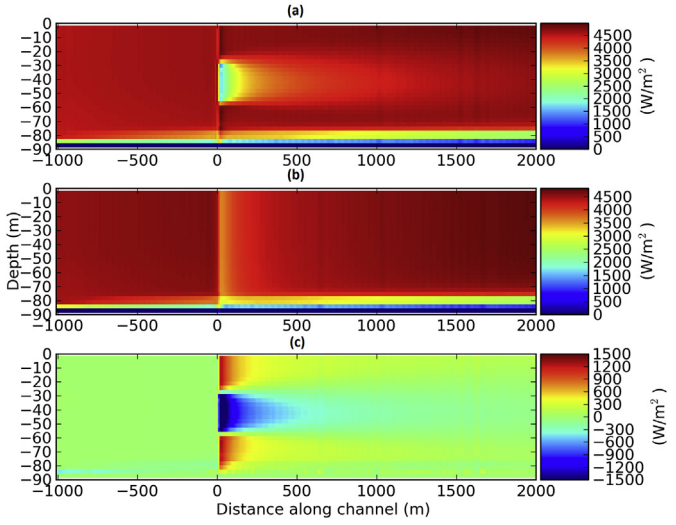

Fig. 6. Power density for (a) the 3-D method, (b) the 2-D method and (c) the power difference between the two methods in a channel of 90 m.

within the Pentland Firth and indeed the Orkney islands are notorious for their complex tidal dynamics and large tidal resource [15,30,50]. The tides in the region are predominantly semi-diurnal; Despite its world leading tidal current speeds, the M_2 amplitude of the vertical tide at the outer-reaches of the Pentland Firth is not remarkable, 1.02 m at Wick (East) and 1.35 m at Scrabster (West). Hence, it is the combination of the 2 h phase difference between the North Atlantic end of the channel and the North Sea end of the channel (see Fig. 7), and the complex geography resulting from the existence of many islands and headlands, which serve to further augment the tidal currents, leading to peak spring current speeds which exceed 4 m/s, making the Pentland Firth a world leading site for tidal energy development [26]. Four sites, with a total capacity of 800 MW, have been leased by the crown estate for development by tidal energy companies (Fig. 8 a), the largest of which is the *Inner Sound* site, a 400 MW site which was leased to MeyGen for development in the last quarter of 2014 [12,25]. The Inner Sound of Stroma is a prominent island channel located between the Scottish mainland and the Isle of Stroma. Here peak spring currents exceed 3.5 m/s. The capacity of the planned tidal energy development within the Inner Sound of Stroma is equal to that of the other three leased sites combined. Depths within the Pentland Firth range from maximum depths in exceedance of 80 m in the main channel to depths of 30 m in the Inner Sound which shoal gradually towards the coastline.

The Carbon Trust [44] predicts that the tidal resource of the Pentland Firth, accounting for constraints on the extraction of tidal energy (i.e: water depth, grid connections, shipping pathways and flow velocity), will make up 30% of the UK's practical energy resource.

6. Application to the Pentland Firth

6.1. Model setup

The Pentland Firth model has a longitudinal resolution of 500 m and a variable latitudinal resolution, approximately equal to 500 m. The model domain extends from 1.3° W to 4° W and from 58.3° N to 60.3° N (Fig. 8). Bathymetry for the Pentland Firth was provided by the *General Bathymetric Chart of the Oceans* (GEBCO) 30 arc second data set. The vertical resolution was defined by 10 sigma layers, providing a resolution of approximately 3 m in the Inner Sound. The model was nested inside a North West European Shelf model which had a resolution of approximately 3 km, with one-way M_2 and S_2 tidal elevation and tidal current forcing at the boundaries. The validation of the outer model (full results not presented here) for the semi-diurnal M_2 and S_2 tidal constituents were 17 cm and 5 cm for amplitude and 2° and 6° for phase when compared with 12 *in-situ* tide gauges. After the initial run without tidal energy extraction (the control), the model was re-run with 2-D and 3-D tidal energy extraction. A 300 MW tidal array was implemented within the area of the Inner Sound leased by the Crown Estate [12].

6.1.1. Model validation

The M_2 and S_2 constituents separated using the harmonic analysis software T_TIDE [33], were compared with 9 tide gauges located around the Orkney domain and the results given in Table 3. Additionally, the depth averaged velocities at three ADCP locations (see Fig. 8 a) were validated following the principal components analysis method prescribed by Boon [8]; (see Fig. 9).

The RMSE for M_2 and S_2 amplitudes were 7 cm and 3 cm and for phase were 13° and 12° with Scatter Index values of less than 10% for S_2 amplitude and phase and $\sim$ 6% and $\sim$ 12% for M_2 amplitude and phase respectively.

The modelled depth averaged current amplitudes and phases were validated using current and direction measurements from three 30 day ADCP deployments. The devices were deployed within the centre channel of the Pentland Firth by Guardline Surveys on behalf of the Navigation and Safety branch of the Maritime and Coastguard Agency. Each mooring is separated by $\sim$ 8 km. As would be expected, the modelled results show much less variability than the observational data. Overall, it is promising to observe that both magnitude and direction are reasonably represented by the model. The RMSE of the tidal current speed amplitudes and phase for the M_2 and S_2 constituents were 21 cm/s, 4 cm/s and 5°, 13° respectively.

6.2. Results for the baseline case

The model was initially applied to a case with no tidal energy extraction, hereafter referred to as the control scenario, in order to understand the residual circulation and theoretical available kinetic energy before tidal energy extraction. The mid-depth 3-D velocities

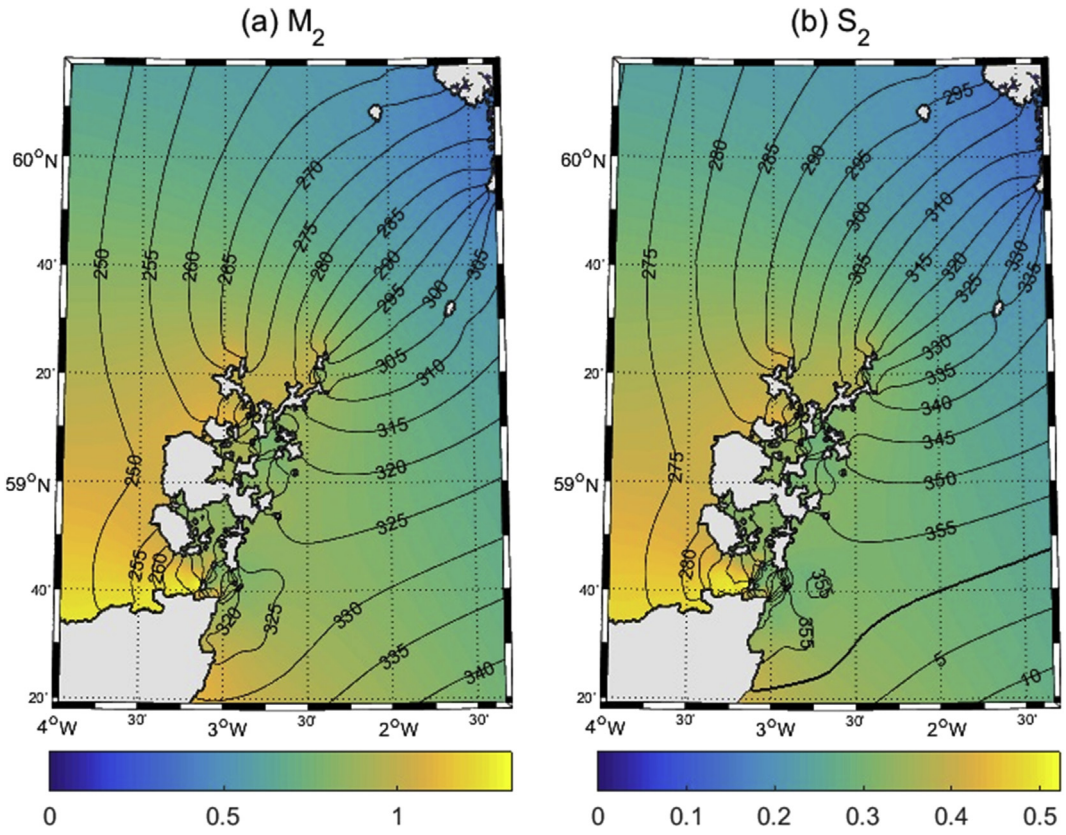

Fig. 7. Orkney model domain. Cotidal lines link locations of equal tidal phase (°) for M_2 (a) and S_2 (b) tidal elevation. The tidal amplitude is indicated by the colour scale (m).

from the regional ocean model were integrated between depths of 10 m and 20 m (the diameter of the turbines) to establish the control scenario flow dynamics. The mapped hub-height integrated velocity field (m/s) shows the streaming of the tide through the Pentland Firth between the islands of Stroma and Swona at different stages of the tide (referenced to Wick), vectors indicate the flow direction (Fig. 10). On the spring flood tide this tidal jet is separated by the Pentland Skerries, behind which an obvious eddy can be identified. The tidal jet of Pentland Skerries doesn't propagate as far on the neap flood tide and the reduced currents in the main channel lead to more resource entering the sub-channels between Stroma and Swona where there is a slight increase of current magnitude. During the ebb phase, the direction of the tidal jet is reversed and fast currents are found at the tip of South Ronaldsay and Dunnet Head. Fig. 8 a, shows the locations of the leased Pentland Firth tidal energy development sites: Brims (A), Brough Ness (B), Ness of Duncansby (C) and Inner Sound (D). In this study, the tidal arrays are located within the Inner Sound of Stroma, shown by the red polygon in Fig. 11. The Inner Sound of Stroma benefits from the increased tidal streaming as a result of channel constraints and subsequently is the most energetic of all the leased tidal stream sites. The residual currents for depth-averaged tidal velocities over a spring-neap cycle display a number of prominent eddies (Fig. 11). The most noteworthy eddies are located in the lee of the Pentland Skerries and the Isle of Stroma.

6.3. Results for the energy extraction cases

The results presented in this section are difference plots between the control scenario and each individual extraction scenario and between the extraction scenarios, i.e. where the tidal energy extraction simulations are individually extracted from the control simulation, and the 3-D simulation is subtracted from the 2-D simulation. In the region of energy extraction, the magnitude of velocity averaged over a spring-neap cycle was reduced by approximately 7 cm/s for the 2-D extraction (Fig. 12a) and 5 cm/s for the 3-D extraction case (Fig. 12b). The change in velocity is greatest in close proximity to the array, however, effects can be seen over the entirety of the model domain as is consistent with other studies [29]. The flow in the main channel of the Pentland Firth is increased by around 5 cm/s, but interestingly, the velocities at the other 3 tidal development zones is reduced. On the whole, the impact on the velocities is greater using 2-D extraction methods than when using the 3-D method (Fig. 12c). The variation in the mean surface, mid-depth and bottom currents is shown in Fig. 13, where every 6th vector is plotted for clarity. In the mid-depths, current speed within the area of the array is 10 cm/s slower for the 3-D case than for the 2-D case, and through the main channel is a 5 cm/s increase in current speeds. In contrast, the surface layers of the water column see a >10 cm/s increase in current speeds within the area of the array. The bottom layer also sees a similar increase in current speed, although not over as large an area, concentrated around the tip of Mell's head. The bottom velocities are constrained by the bottom drag coefficient, hence a much smaller change in velocity is observed in this layer than in the surface layer. The vectors show differences between the methods in the current directions and eddy fields within the Inner Sound, for the surface and bottom layers of the water column. The percentage difference in bed shear stress between the methods is calculated and differences less than 10% are masked out (Fig. 14). Positive values indicate regions where bed shear stresses are greater for the 3-D scenario. The resultant pattern is complex and highlights the non-linearities between the interaction of the hydrodynamics and the tidal array. Overall, the 3-D extraction scenario leads to higher bed shear

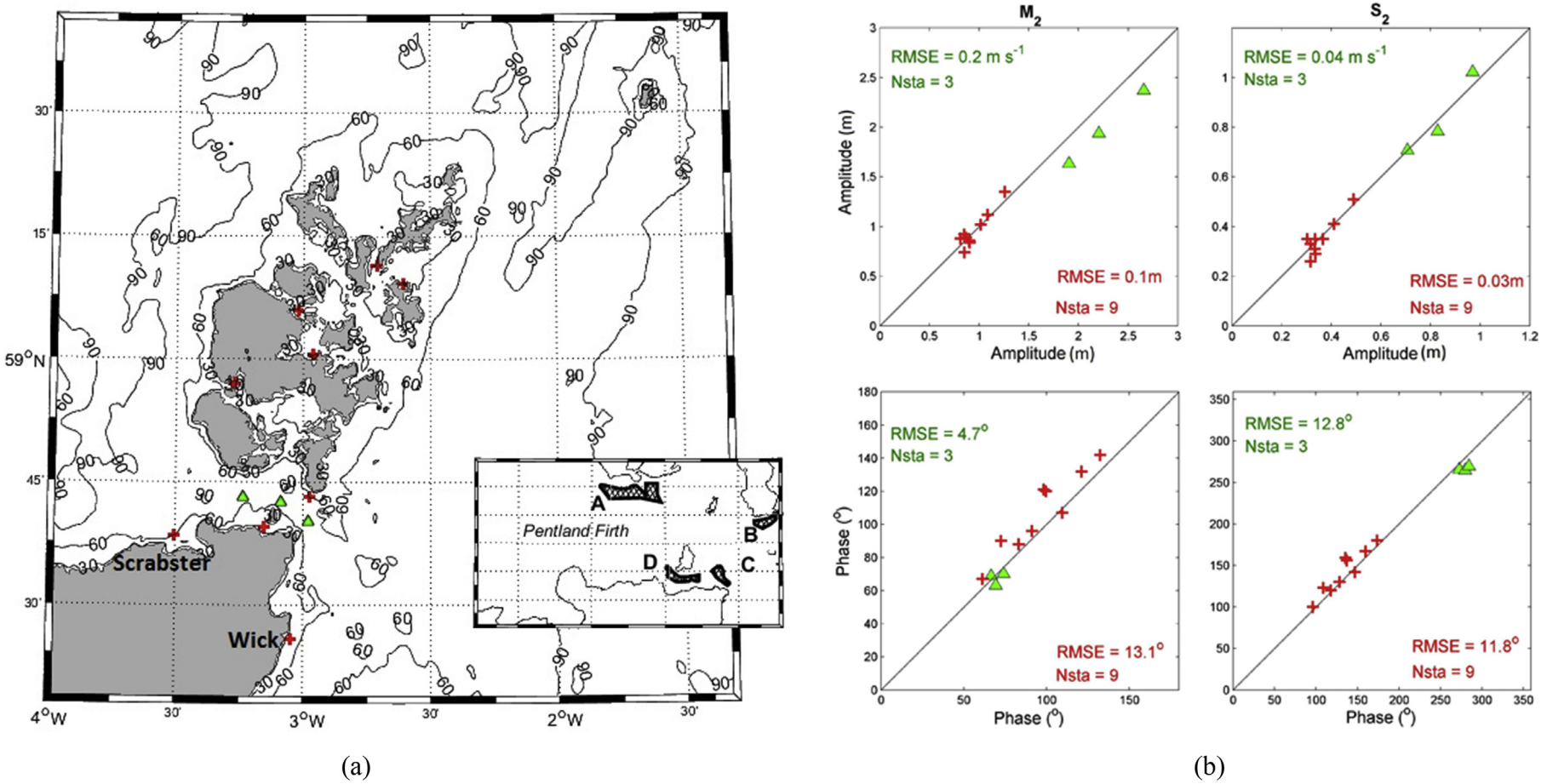

Fig. 8. (a) Orkney model domain showing ADCP locations (green triangles), tide gauge locations (red crosses). Inset is the Pentland Firth with polygons displaying the regions allocated by the crown estate for tidal energy development. Bathymetry contours show spatial distribution of water depth over the model grid. (b) Comparison of modelled (x) and observed (y) M_2 and S_2 amplitudes and phases for velocity (green triangles) and elevation (red crosses). (For interpretation of the references to colour in this figure legend, the reader is referred to the web version of this article.)

Table 3
Observed and modelled amplitudes (H, in meters) and phases (g, in degrees) of the M_2 and S_2 tidal constituents for the 9 tide gauges represented by red crosses in Fig. 8. The principle tide gauge is identified in bold font.

Station	Observed				Modelled			
	M2		**S2**		**M2**		**S2**	
	H (m)	g (°)	H (m)	g (°)	H (m)	g (°)	H (m)	g (°)
Wick	**1.02**	**322**	**0.35**	**0**	**1.02**	**312.31**	**0.37**	**353.51**
Burwick	0.88	287	0.35	322	0.81	289.39	0.30	326.77
Gills Bay	1.12	268	0.41	300	1.09	263.14	0.41	297.77
Scrabster	1.35	247	0.51	280	1.26	241.25	0.49	276.01
Kirkwall	0.84	301	0.29	339	0.91	278.26	0.34	315.64
Loth	0.74	300	0.26	336	0.85	279.67	0.32	316.96
Kettletoft Pier	0.92	312	0.33	347	0.85	301.24	0.32	339.69
Tingwall	0.86	276	0.31	310	0.90	271.16	0.33	308.22
Stromness	0.89	270	0.35	303	0.87	252.43	0.34	288.56
RMSE					**0.07**	**13.06**	**0.03**	**11.83**
SI(%)					**6.39**	**12.13**	**9.11**	**8.24**

stresses than the 2-D extraction scenario.

7. Discussion

A 3-D ROMS model has been used to compare tidal energy extraction modelling techniques and highlight the importance of using 3-D models for resource assessments. To simulate depth-averaged tidal energy extraction techniques within a 3-D ROMS model, a scaled thrust force is applied over the entirety of the water column at a single location within an idealised channel. For 3-D tidal extraction, a method originally developed and validated by Roc et al. [38] for ROMS is used. Here the turbine thrust force is applied over a vertical region of the water-column characterised by the diameter of the turbine, located at the mid-point of the water column at a single location within an idealised channel. The idealised channel experiment ensured that both techniques were comparable and led to the same reduction of velocity across the turbine area. After which both methods were applied to the leased Inner Sound development zone within a regional model of the Pentland Firth. The control Pentland Firth scenario was validated using ADCP and tide gauge measurements throughout the domain. The validation results show that the model errors for amplitude and phase are less than 10% of the tidal regime, and is thus considered suitable to compare tidal array modeling methods.

Our comparison of tidal energy extraction modeling techniques reveals that using a 2-D method to extract energy from the water column leads to a misrepresentation of the surface and bottom flow fields (Fig. 3). The flow beneath the turbine is of particular importance as it is constrained between the turbine and seabed so could

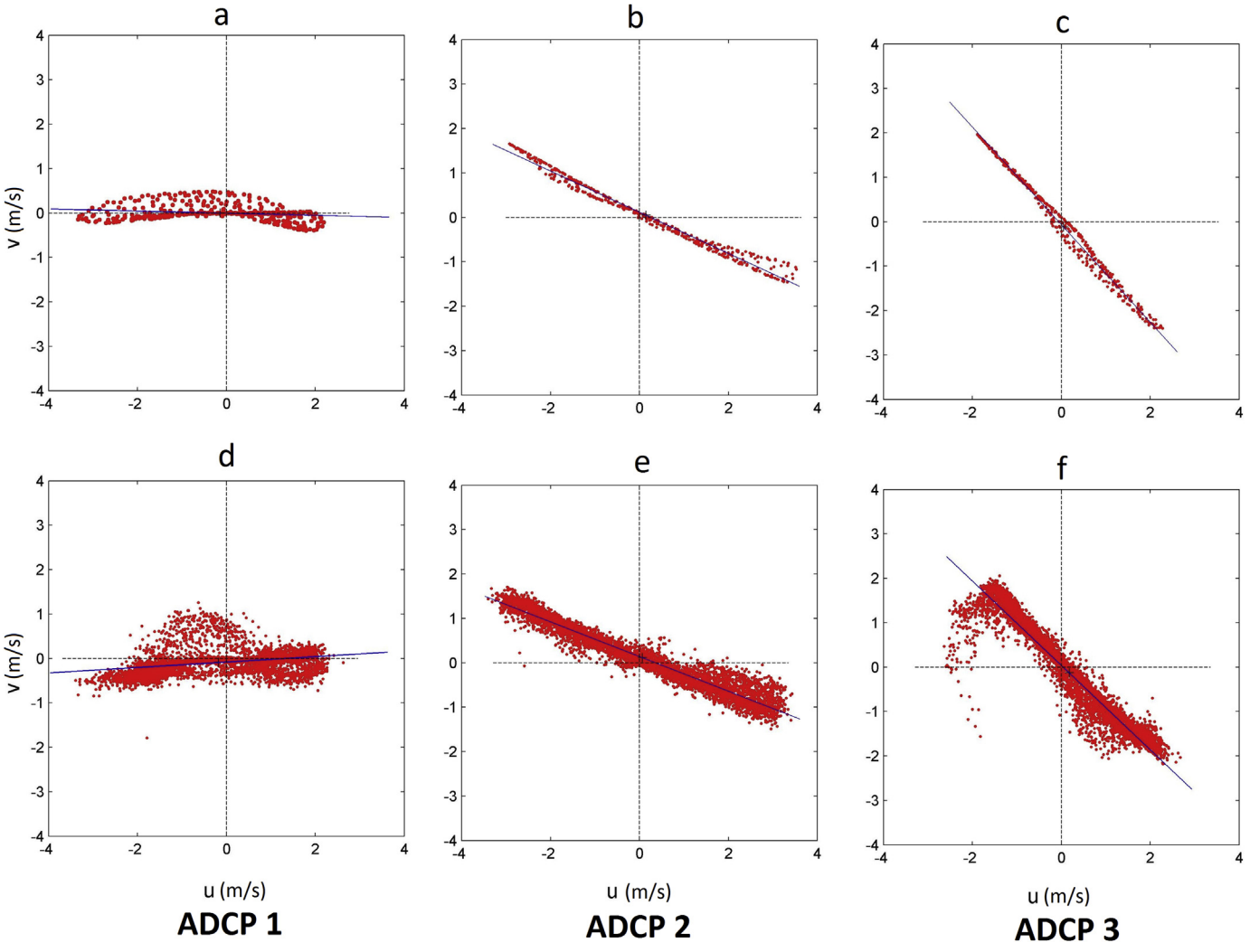

Fig. 9. Tidal ellipses for the modelled (a,b and c) and observed (d, e and f) tidal currents at each ADCP location.

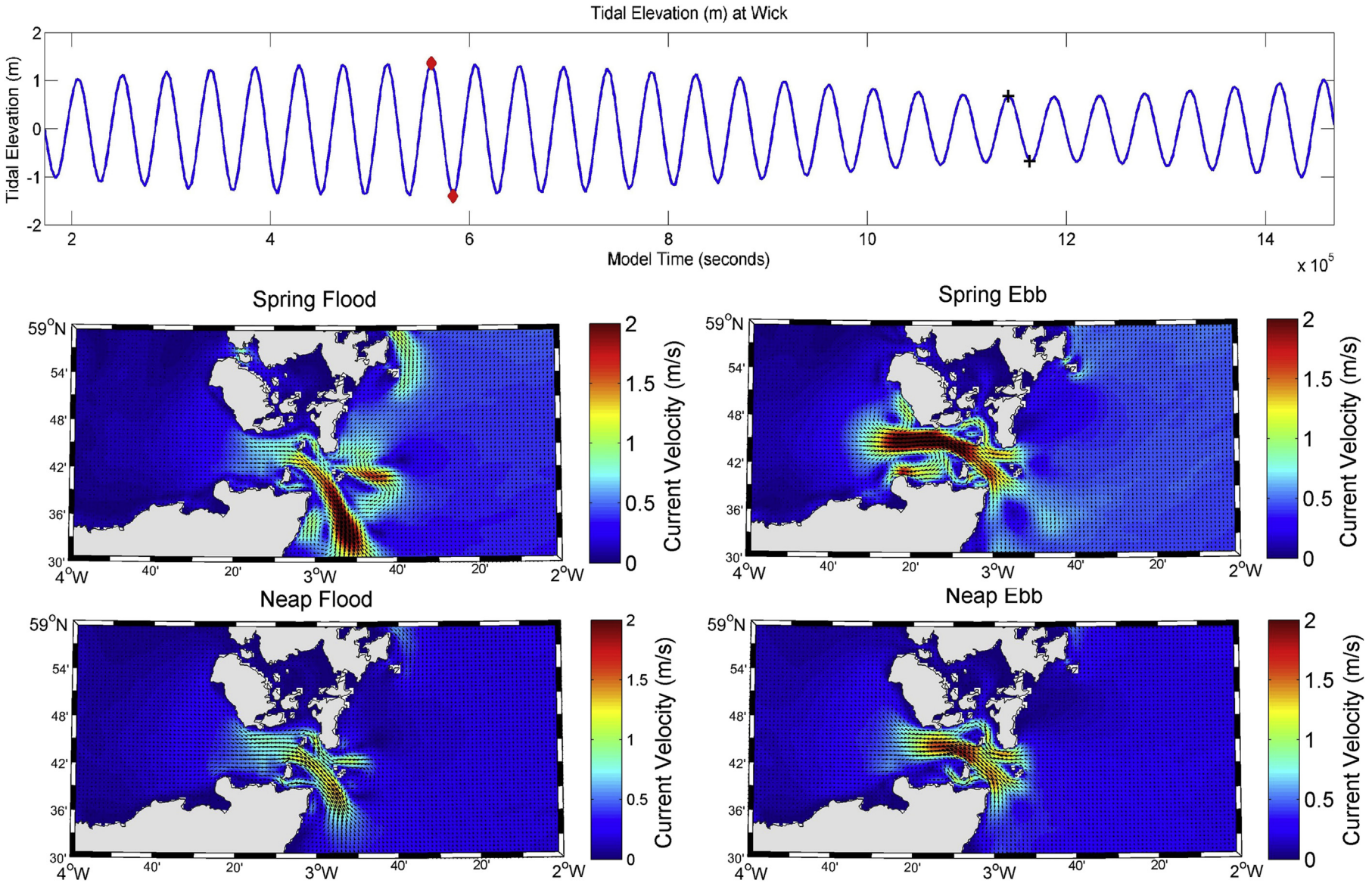

Fig. 10. Tidal streaming within the Pentland Firth when it is peak spring flood and ebb tides (red diamonds) and neap flood and ebb tides (black cross) at Wick. Colours show velocity magnitude at the mid-depth, and vectors show current direction. (For interpretation of the references to colour in this figure legend, the reader is referred to the web version of this article.)

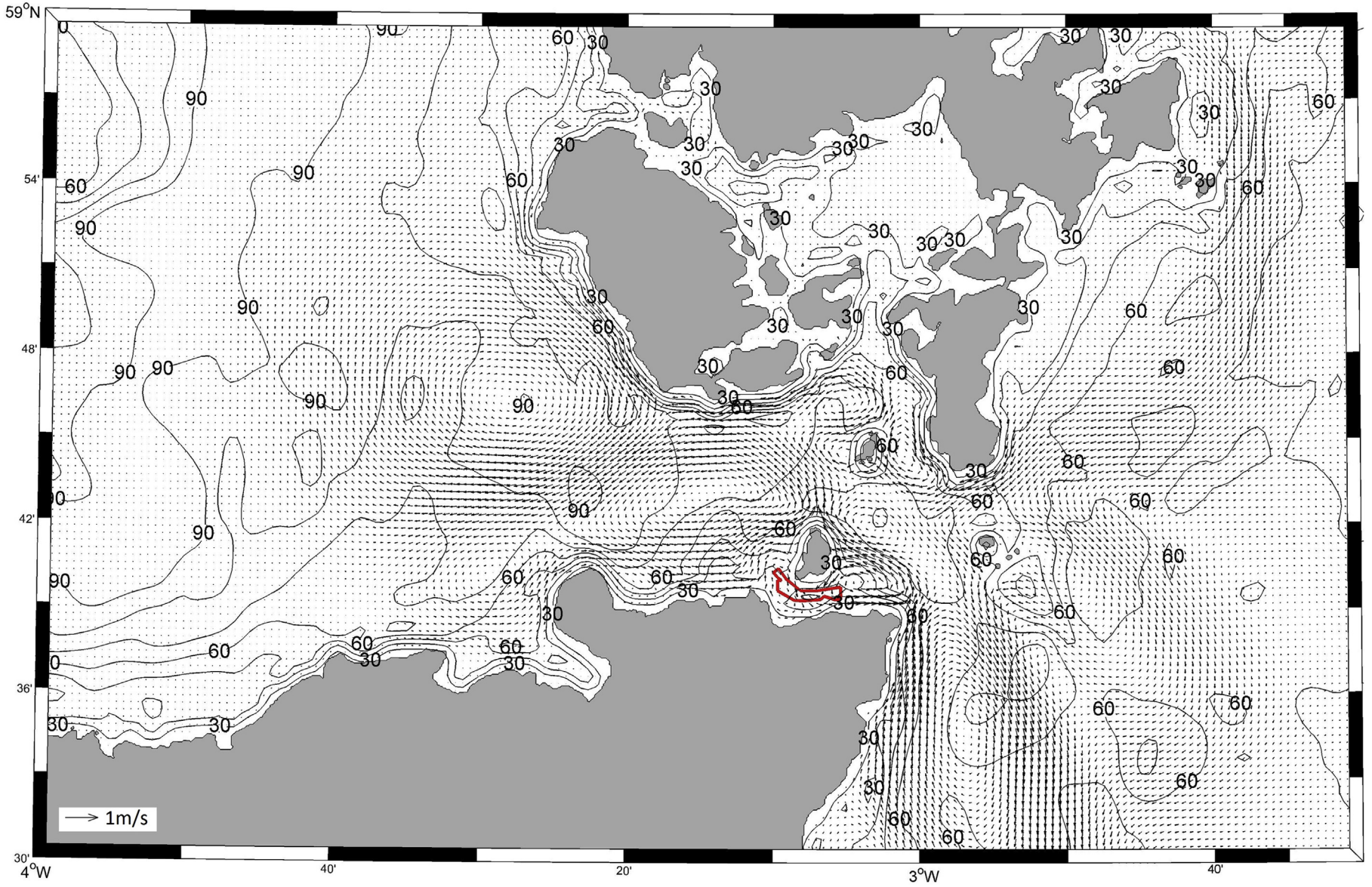

Fig. 11. Modelled residual tidal currents in the Pentland Firth for the control scenario. The red polygon indicates the location of the Inner Sound tidal array and the contours represent the water depth (m). (For interpretation of the references to colour in this figure legend, the reader is referred to the web version of this article.)

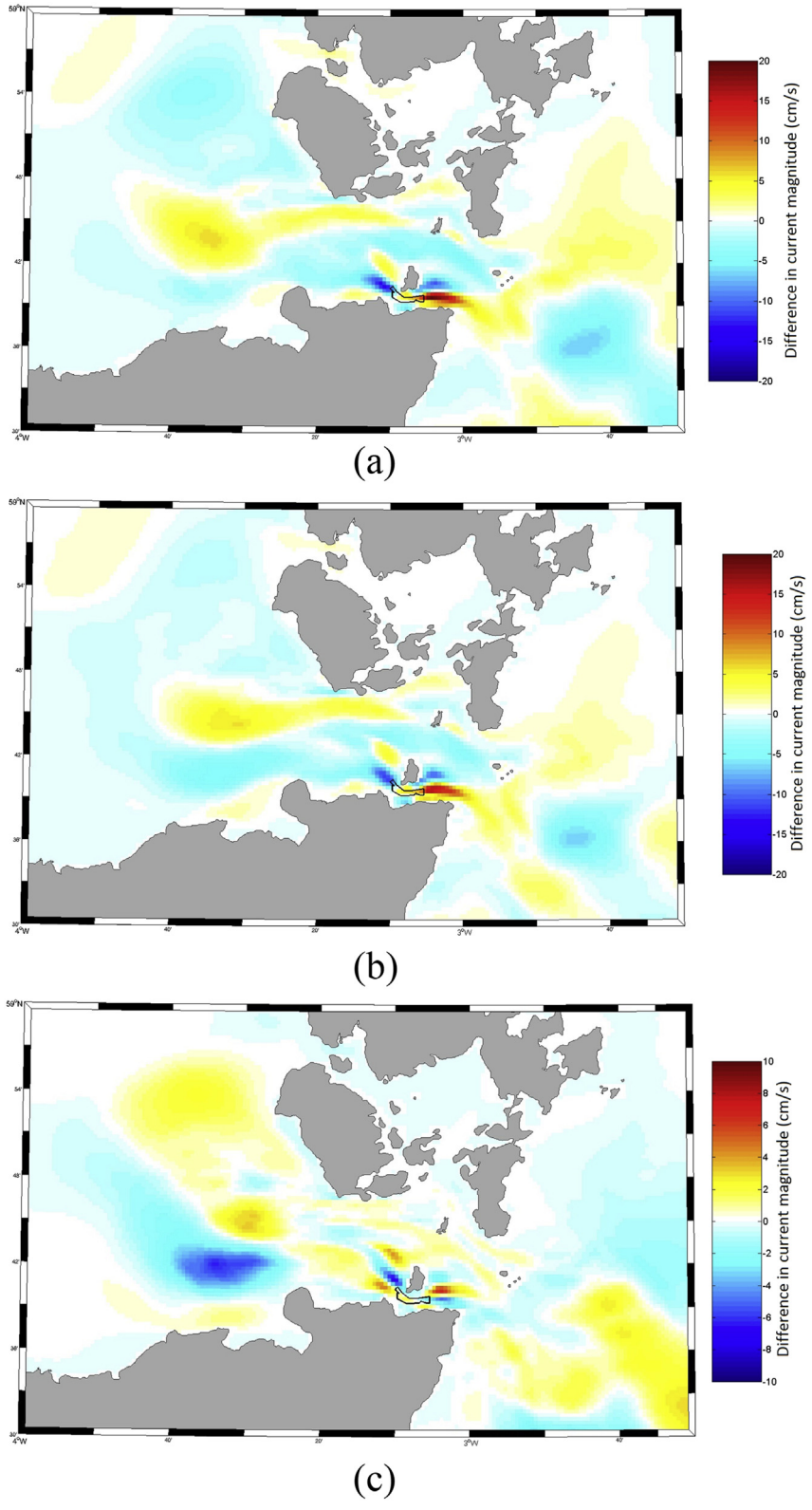

Fig. 12. Change in magnitude of velocity (cm/s), due to energy extraction over a spring-neap cycle between (a) the control and 2-D extraction scenario, (b) the control and 3-D extraction scenario and (c) 2-D and 3-D extraction scenarios. Black polygon shows the location of the turbine array for each case.

have quite considerable implications for sediment transport investigations (i.e. [17]). Little research has been published on wave-current interaction around tidal arrays however it is understood that incoming wave direction could have quite a significant impact on tidal resource so efforts made to implement 3-D tidal energy extraction would reduce uncertainty in these estimations [21,22].

The results from the idealised channel model suggest that depth-averaged models can be misleading, when the depth

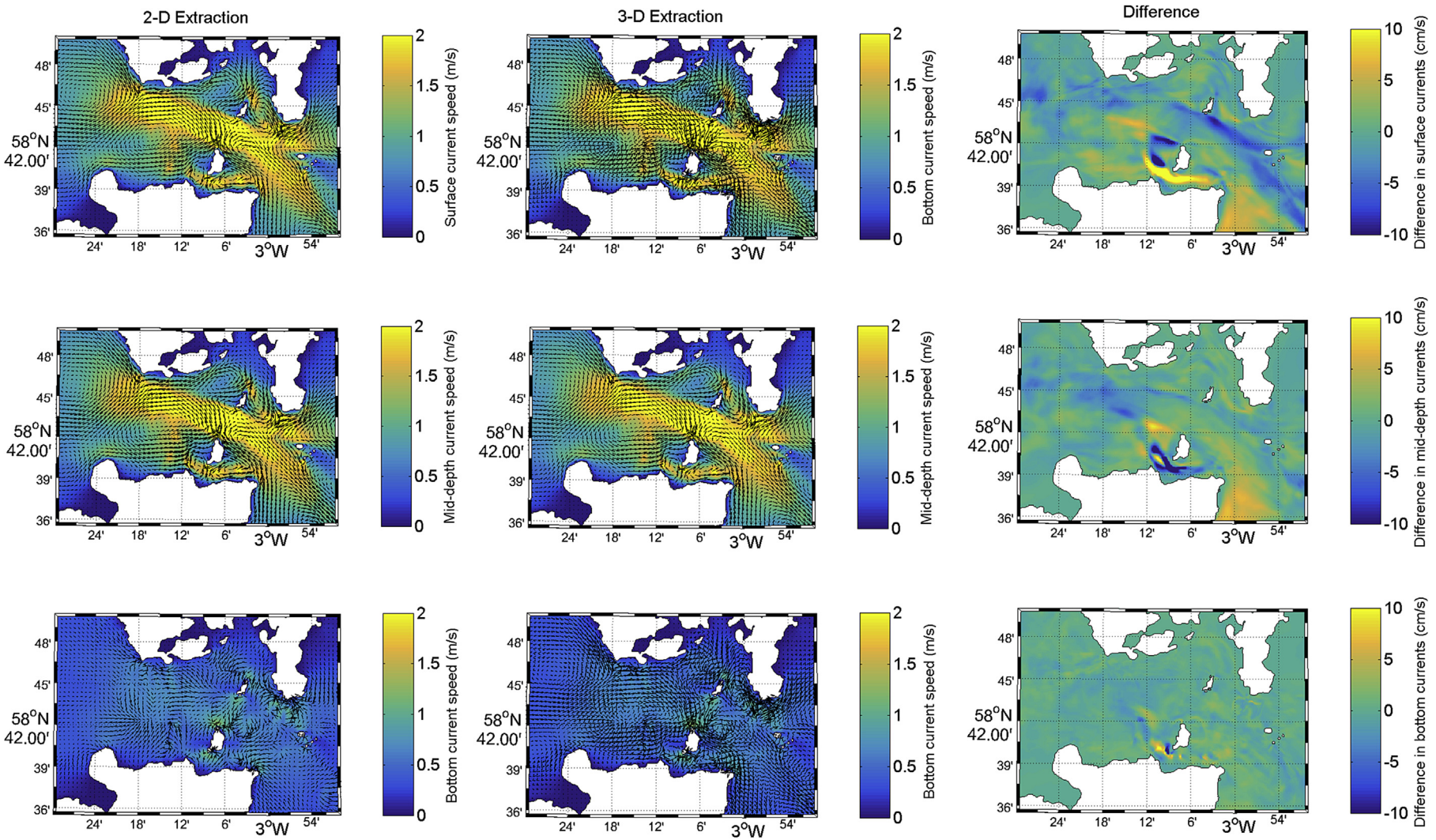

Fig. 13. Comparison of mean surface, mid-depth and bottom currents for 2-D and 3-D extraction simulations.

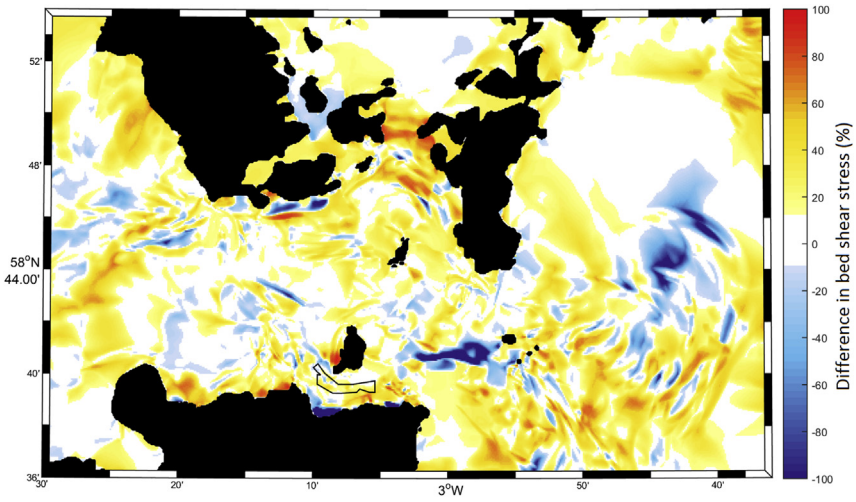

Fig. 14. Percentage change in magnitude of bed shear stress between 3-D and 2-D extraction scenarios over a spring-neap cycle. Black polygon shows the location of the turbine array.

averaged velocities are compared for both methods, both methods appear to reduce the tidal flow by an identical amount (Fig. 2). However, upon comparing the 3-D profiles, the velocity reduction in the location of the turbine is much greater, suggesting an uncertainty in resource assessments between 20% and 25% (Table 2; Fig. 3). Traditional 2-D extraction methods where an increased frictional force is applied at the sea-bed cause the near-bed velocity to reduce, this is not the case with the actuator disc method where the velocities will increase as they by-pass the region of extraction. Future generations of tidal energy development are likely to look to deeper water environments and 3-D modelling techniques will be vital for reducing the uncertainty in resource assessments.

Located below the main residual circulation patterns (Fig. 11) within the channel are a number of sandbanks [10]. Sandbanks are of significant importance to shallow water regions where their presence enhances wave dissipation and refraction which in some cases provides natural protection to the shoreline [29,14,23]. In some regions they are of significant economical importance and these quiescent regions can provide important feeding grounds for fish and have high ecological significance for benthic communities [51]. Understanding how these regions might change as a result of tidal stream energy extraction is subsequently of high importance and will be the emphasis of future work.

Although the Pentland Firth is a channel and thus might be expected to have rectilinear currents, some misalignment and flow asymmetry can be observed, as hypothesised by Lewis et al. [24] (Fig. 10). Interestingly, for both extraction scenarios, there is asymmetry in the flow behavior either side of the Inner Sound. We see a decrease in flow propagating out of the Inner Sound into the North Sea, however, a clear increase in flow can be seen either side of the array particularly where it becomes constrained between the array and the coastline (Fig. 12). Extraction of energy in regions of tidal asymmetry has been shown to have a greater impact on sediment transport than areas where flood and ebb tides are symmetrical [28]. Extracting energy from the Inner Sound affects the current magnitude at the other three sites within the Pentland Firth - a more detailed study into the changes to hydrodynamics at these sites will be required to fully characterise the effect on the resource. 3-D energy extraction methods will help improve the quantification of the impact of tidal energy extraction on sea-bed processes (Fig. 3; [5]).

A number of studies have established that small tidal stream developments are likely to have a minimal effect on sediment dynamics [36,17]. The 3-D extraction case had a greater impact on the velocities within the vicinity of the array, however the 2-D method appears to remove more kinetic energy from the domain (Fig. 12). Studies seeking optimal turbine array design tend to settle upon a tidal fence design (i.e. [2]), the increased levels of extraction and impacts on flow from these arrays will have a greater impact on the flow dynamics than those presented here. Nevertheless, from Fig. 13, if we consider the velocities within the bottom most depth layer, the 3-D method has the fastest near-bed velocities during the flood tide by a margin exceeding 10 cm/s. Bed shear stresses are related to velocity squared and thus justifies the importance of defining the turbines as a mid-depth force-term [43].

This research provides a comparison of the methods used to model tidal energy extraction in regional models, nevertheless further research would be required to quantify the error between resource assessment models. Further questions remain as to whether device resolving methods are appropriate within regional models, this would involve improvements to model efficiency and resolution to take into account turbine array design and turbine induced turbulence. There is a clear knowledge gap with regards to feedbacks between tidal stream devices and regional hydrodynamics, since little observational data is available for the validation of device resolving models. Additionally, there are many ways in which modelling the resource could be improved, taking into account the interaction of waves with the tidal stream resource and array development, and the consequences of tidal energy developments upon neighboring tidal energy development sites. These additions would come at a high computational cost but one which is within the realm of current high performance computing technology.

8. Conclusions

Although observational measurements are key for model validation and for characterising the resource, they are costly and unable to account for spatial variations. Hence, numerical modelling tools are essential within the tidal energy industry for resource and environmental impact assessments.

We find a 3-D modeling approach is necessary to resolve vertical flow bypass around the turbine and are therefore key to reducing bias in resource and environmental impact assessments. Using the 3-D method, velocities across the extraction region are between 20% and 25% less than they are for the 2-D method. This research

showed that as water depth increased the discrepancy in velocity at the disk between the two methods also increased, suggesting that there are greater uncertainties associated with resource assessments with 2-D models in deeper water. Additionally it was found that velocities between the turbine and the sea bed for the 3-D method exceed those in the same region for the 2-D method by more than 10%, suggesting that depth-averaged models assessing the impacts on sediment pathways could be greatly underestimating the levels of sediment transport. Moreover, the vertical structure of the flow is essential to resolve to reduce uncertainties within power calculations, particularly where water depths exceed 30 m. Therefore, depth-averaged models - which are computationally more efficient - are useful tools for a first order of approximation of resource but for accurate assessments of resource interaction with tidal devices 3-D models are required. The use of 3-D models will further reduce the uncertainty in physical environmental impact assessments which would aid the development of the tidal stream industry.

Acknowledgements

Alice Goward Brown wishes to acknowledge Fujitsu and HPC Wales for their role in funding and providing computational support throughout this PhD research. Simon Neill and Matt Lewis would like to acknowledge the support of the Sêr Cymru National Research Network for Low Carbon, Energy and the Environment (NRN-LCEE) project QUOTIENT. ADCP data for model validation was kindly provided by the University of Highlands and Islands Environmental Research Institute.

References

[1] T.A. Adcock, S. Draper, T. Nishino, Tidal power generation—a review of hydrodynamic modelling, Proc. Inst. Mech. Eng. Part A J. Power Energy (2015), 0957650915570349.
[2] T.A. Adcock, S. Draper, G.T. Houlsby, A.G. Borthwick, S. Serhadlolu, The available power from tidal stream turbines in the Pentland Firth, Proc. R. Soc. A Math. Phys. Eng. Sci. 469 (2157) (2013).
[3] R. Ahmadian, R. Falconer, B. Bockelmann-Evans, Far-field modelling of the hydro-environmental impact of tidal stream turbines, Renew. Energy 38 (1) (2012) 107—116.
[5] A.S. Bahaj, L.E. Myers, M.D. Thomson, N. Jorge, Characterising the wake of horizontal axis marine current turbines, in: Proc. 7th EWTEC, 2007.
[6] S. Baston, R.E. Harris, D.K. Woolf, R.A. Hiley, J.C. Side, Sensitivity analysis of the turbulence closure models in the assessment of tidal energy resource in Orkney, in: 10th European Wave and Tidal Energy Conference, Aalborg, Denmark, 2013.
[7] L. Blunden, A. Bahaj, Tidal energy resource assessment for tidal stream generators, Proc. Inst. Mech. Eng. Part A J. Power Energy 221 (2) (2007) 137—146.
[8] J.D. Boon, Secrets of the Tide: Tide and Tidal Current Analysis and Applications, Storm Surges and Sea Level Rise, Horwood Publishing, Chichester (UK), 2004.
[9] I. Bryden, G.T. Melville, Choosing and evaluating sites for tidal current development, Proc. Inst. Mech. Eng. Part A J. Power Energy 218 (8) (2004) 567—577.
[10] I.G. Bryden, S.J. Couch, A. Owen, G. Melville, Tidal current resource assessment, Proc. Inst. Mech. Eng. Part A J. Power Energy. ISSN: 0957-6509 221 (2) (2007) 125—135, 2041-2967.
[11] S.J. Couch, I. Bryden, Tidal current energy extraction: hydrodynamic resource characteristics, Proc. Inst. Mech. Eng. Part M J. Eng. Marit. Environ. 220 (4) (2006) 185—194.
[12] Crown Estate, Leasing round and projects, URL: http://www.thecrownestate.co.uk, 2010.
[13] S. Draper, G. Houlsby, M. Oldfield, A. Borthwick, Modelling tidal energy extraction in a depth-averaged coastal domain, IET Renew. power Gener. 4 (6) (2010) 545—554.
[14] K.R. Dyer, D.A. Huntley, The origin, classification and modelling of sand banks and ridges, Cont. Shelf Res. 19 (10) (1999) 1285—1330.
[15] M. C. Easton, D. K. Woolf, P. A. Bowyer, The dynamics of an energetic tidal channel, the Pentland Firth, Scotland, Cont. Shelf Res.
[17] I. Fairley, I. Masters, H. Karunarathna, The cumulative impact of tidal stream turbine arrays on sediment transport in the Pentland Firth, Renew. Energy 80 (2015) 755—769.
[18] M. Harrison, W. Batten, L. Myers, A. Bahaj, Comparison between CFD simulations and experiments for predicting the far wake of horizontal axis tidal turbines, Renew. Power Gener. IET 4 (6) (2010) 613—627.
[19] M.E. Harrison, W.M.J. Batten, L.E. Myers, A.S. Bahaj, A comparison between CFD simulation and experiments for predicting the far wake of horizontal axis tidal turbines, in: 8th European Wave and Tidal Energy Conf, Uppsala, Sweden, 2009.
[21] M.R. Hashemi, S.P. Neill, P.E. Robins, A.G. Davies, M.J. Lewis, Effect of waves on the tidal energy resource at a planned tidal stream array, Renew. Energy 75 (2015) 626—639.
[22] M. Lewis, S. Neill, M. Hashemi, M. Reza, Realistic wave conditions and their influence on quantifying the tidal stream energy resource, Appl. Energy 136 (2014a) 495—508.
[23] M. Lewis, S. Neill, A. Elliott, Interannual variability of two offshore sand banks in a region of extreme tidal range, J. Coast. Res. 31 (2) (2014b) 265—275.
[24] M. Lewis, S. Neill, P. Robins, M. Hashemi, Resource assessment for future generations of tidal-stream energy arrays, Energy 83 (2015) 403—415.
[25] MeyGen, UK leads marine energy revolution as worlds largest tidal stream project agrees investment to begin construction in Scotland, URL: http://www.meygen.com/the-project/meygen-news/, 2010.
[26] R.O. Murray, A. Gallego, A modelling study of the tidal stream resource of the Pentland Firth, Scotland, Renew. Energy 102 (2017) 326—340.
[27] L. Myers, A. Bahaj, Simulated electrical power potential harnessed by marine current turbine arrays in the Alderney Race, Renew. Energy 30 (11) (2005) 1713—1731.
[28] S. Neill, E. Litt, S. Couch, A. Davies, The impact of tidal stream turbines on large-scale sediment dynamics, Renew. Energy 34 (12) (2009) 2803—2812.
[29] S.P. Neill, J.R. Jordan, S.J. Couch, Impact of tidal energy converter (TEC) arrays on the dynamics of headland sand banks, Renew. Energy 37 (1) (2012) 387—397.
[30] S. P. Neill, A. Vögler, A. J. Goward-Brown, S. Baston, M. J. Lewis, P. A. Gillibrand, S. Waldman, D. K. Woolf, The wave and tidal resource of Scotland, Renew. Energy.
[31] J.C. Ohlmann, S. Mitarai, Lagrangian assessment of simulated surface current dispersion in the coastal ocean, Geophys. Res. Lett. 37 (17) (2010).
[32] S.D.G.H.M. Oldfield, A. Borthwick, Modelling tidal energy extraction in a depth-averaged coastal domain.
[33] R. Pawlowicz, B. Beardsley, S. Lentz, Classical tidal harmonic analysis including error estimates in MATLAB using T_TIDE, Comput. Geosci. 28 (8) (2002) 929—937.
[34] B. Polagye, J. Epler, J. Thomson, Limits to the predictability of tidal current energy, in: OCEANS 2010, IEEE, 2010, pp. 1—9.
[35] D. Prandle, The vertical structure of tidal currents and other oscillatory flows, Cont. Shelf Res. 1 (2) (1982) 191—207.
[36] P.E. Robins, S.P. Neill, M.J. Lewis, Impact of tidal-stream arrays in relation to the natural variability of sedimentary processes, Renew. Energy 72 (2014) 311—321.
[37] P.E. Robins, S.P. Neill, M.J. Lewis, S.L. Ward, Characterising the spatial and temporal variability of the tidal-stream energy resource over the northwest European shelf seas, Appl. Energy 147 (2015) 510—522.
[38] T. Roc, D.C. Conley, D. Greaves, Methodology for tidal turbine representation in ocean circulation model, Renew. Energy. ISSN: 09601481 51 (2013) 448—464.
[39] M. Sánchez, R. Carballo, V. Ramos, G. Iglesias, Tidal stream energy impact on the transient and residual flow in an estuary: a 3D analysis, Appl. Energy 116 (2014) 167—177.
[40] G. Shapiro, Effect of tidal stream power generation on the region-wide circulation in a shallow sea, Ocean Sci. 7 (2011) 165—174.
[41] A.F. Shchepetkin, J.C. McWilliams, The regional oceanic modeling system (ROMS): a split-explicit, free-surface, topography-following-coordinate oceanic model, Ocean Model. 9 (4) (2005) 347—404.
[42] M.A. Shields, D.K. Woolf, E.P. Grist, S.A. Kerr, A.C. Jackson, R.E. Harris, M.C. Bell, R. Beharie, A. Want, E. Osalusi, Marine renewable energy: the ecological implications of altering the hydrodynamics of the marine environment, Ocean Coast. Manag. 54 (1) (2011) 29.
[43] R. Soulsby, Dynamics of Marine sands: a Manual for practical Applications, Thomas Telford, 1997.
[44] The Carbon Trust, Tech. Rep., 2011.
[45] K. Thyng, J. Riley, Idealized headland simulation for tidal hydrokinetic turbine siting metrics, in: OCEANS 2010, IEEE, vol. 16, 2010.
[46] C. Vogel, R. Willden, G. Houlsby, A correction for depth-averaged simulations of tidal turbine arrays, in: Proceedings of the 10th European Wave and Tidal Energy Conference (EWTEC), Aalborg, Denmark, vol. 25, 2013.
[47] J. Warner, B. Armstrong, R. He, J. Zambon, Development of a coupled Ocean atmosphere wave sediment transport (COAWST) modeling system, Ocean Model. 35 (3) (2010) 230—244.
[48] J. Whelan, J. Graham, J. Peiro, A free-surface and blockage correction for tidal turbines, J. Fluid Mech. 624 (2009) 281—291.
[49] Z. Yang, T. Wang, A.E. Copping, Modeling tidal stream energy extraction and its effects on transport processes in a tidal channel and bay system using a three-dimensional coastal ocean model, Renew. Energy 50 (2013) 605613.
[50] S.P. Neill, M.R. Hashemi, M.J. Lewis, The role of tidal asymmetry in characterizing the tidal energy resource of Orkney, Renew. Energy 68 (2014) 337—350.
[51] A. Chatzirodou, H. Karunarathna, Impacts of tidal energy extraction on sea bed morphology, Coast. Eng. Proc. 1 (34) (2014) 33.